Examining the Oxidation States of Metals in Aerosols Emitted by Electronic Cigarettes

Kashala Fabrice Kapiamba,[1] Stephen Yaw Owusu,[2] Yangtao Wu,[3] Yue-Wern Huang,[4] Yi Jiang,[3] Yang Wang[1, *]

[1]Department of Chemical, Environmental, and Materials Engineering, University of Miami, Miami, FL, 33146, USA

[2]Department of Chemistry, Missouri University of Science and Technology, Rolla, MO, 65409, USA

[3]Department of Civil and Environmental Engineering, The Hong Kong Polytechnic University, Hung Hom, Kowloon, Hong Kong

[4]Department of Biological Sciences, Missouri University of Science and Technology, Rolla, MO, 65409, USA

Submitted to:

ACS Chemical Research in Toxicology

* To whom correspondence should be addressed:

Tel: +1 (305) 284-3323

E-mail address: yangwang@miami.edu

TOC graphic

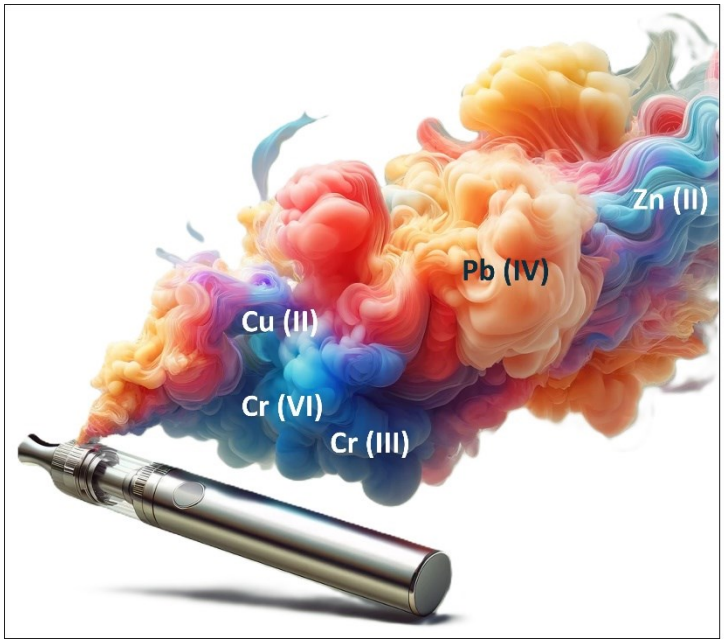

Abstract

Electronic cigarettes (ECs) emit many toxic substances, including metals, that can pose a threat to users and the environment. The toxicity of the emitted metals depends on their oxidation states. Hence, this study examines the oxidation states of metals observed in EC aerosols. X-ray photoelectron spectroscopy (XPS) analysis of the filters that collected EC aerosols identified the oxidation states of five primary metals (based on surface sample analysis), including chromium (III) (close to 100 %) under low power setting while a noticeable amount of chromium (VI) (15%) at higher power settings of the EC; and copper (II) (100 %), zinc (II) (100 %), nickel (II) (100 %), and lead (II) (65 %) and lead (IV) (35 %) regardless of power settings. This observation indicates that the increased temperature due to higher power settings could alter the oxidation states of certain metals. We noted that many metals were in their lesser toxic states; however, inhaling these metals may still pose health risks.

Keywords: Electronic cigarette (EC), aerosol, metal, oxidation states, inhalation toxicity.

1. Introduction

Since their invention in the early 2000s, electronic cigarettes (ECs) have been promoted as an alternative means of quitting smoking and avoiding inhaling toxic substances.[1,2] However, studies on EC smoke have confirmed the presence and, in some instances, high levels of similar toxic substances found in tobacco cigarette smoke.[3–6] The toxic levels of aldehydes, including diacetyl, acetoin, acetaldehyde, and formaldehyde, in several brands of ECs have been reported.[7,8] These carbonyls are generated by the thermal and catalytic degradation of propylene glycol (PG) and, to some extent, vegetable glycerin (VG), the main components in the e-liquid. Metals have also been detected in EC aerosols. In a systematic review, Zhao et al.[9] identified 24 studies on metals/metalloids in e-liquids, EC aerosols, and human biosamples of EC users. These studies confirmed the presence of unsafe levels of Al, As, Cd, Co, Cr, Cu, Fe, Mn, Ni, Pb, Sb, Se, Sn, and Zn.[3,6,9,10]

The emission of metal nanoparticles from ECs is of concern because of their potent toxicity at low concentrations, even on the nanogram scale per puff of smoke.[6] Our recent analysis of metals in EC primary and secondhand aerosols revealed relatively higher concentrations of five metals (Cr, Cu, Mn, Ni, and Zn), some of which exceed the safe daily limits proposed by the National Institute for Occupational Safety & Health and the European Medicines Agency.[11] Toxic levels of metals can impair normal physiological functions and lead to diseases such as neurodegenerative disorders and cancer.[12] For instance, occupational exposure to Ni by industrial workers may induce toxicity in the respiratory tract, lungs, and immune system.[13] Exposure to Zn is prominent in galvanized sheet steel processing plants. Inhalation of a mixture of particles and fumes, including ZnO, induces an increase in some airway pro-inflammatory markers (IL-8, MMP-9, and TIMP-1).[14] Copper oxide nanoparticles

have been used as antimicrobials, and concerns have been raised regarding their toxicity, including their effects on the immune system and blood.[15,16] Inhalation of these nanoparticles leads to significant immune response modulation, including lymphocyte activation and impaired phagocytic activity of granulocytes, coupled with a reduction in important antioxidants like reduced glutathione. Additionally, prolonged exposure disrupts key biological processes and pathways, such as collagen formation, immune response, and cell cycle, and induces apoptotic processes, potentially implicating roles in carcinogenesis.[15,17] Recently, researchers have examined ECs toxicity in greater detail via *in vivo* and *in vitro* studies.[16–18] In addition, the toxicity (e.g., airway inflammation, pulmonary cell response) of metals detected in EC aerosols, including Pb and Zn, has been reported in several publications.[14,15,19–22]

The adverse effects of various metals largely depend on their oxidation states.[23,24] For example, Cr (VI) is toxic and carcinogenic at a very low dose, while Cr (III) may pose potential risks, such as asthma, dermatitis, and rhinitis when inhaled.[25] The solubility disparity between Cr (III) and Cr (VI) compounds significantly influences their absorption rates. While chromate, in the form of Cr (VI), exhibits high solubility in the form of Cr (VI), Cr (III) oxide is less soluble and requires gradual chelation for dissolution.[26] Furthermore, in pulmonary environments, the presence of ascorbic acid within the surfactant fluid facilitates the rapid reduction of Cr (VI) to Cr (III). This reduction process contributes to the accumulation of low Cr concentrations in the lungs, with an approximate half-life of 5 years.[27,28] A second instance is Mn, which can exist as Mn (II) or Mn (III) oxidation states, with Mn (III) as the primary source of cell toxicity.[29] The toxicity of Mn is known to be caused by its accumulation in the mitochondria, where superoxide oxidizes Mn (II) to Mn (III).[30] A third example is Cu, which can exist in Cu (I), Cu (II) or even the intermediate Cu (III), and of these states, Cu (I) is known as the most toxic form.[31,32]

As the metals observed in EC smoke may have varying toxicity levels depending on their oxidation states, it is necessary to examine their oxidation states to improve our understanding of the adverse effects associated with EC usage.[23] Herein, we examined the oxidation states of metals in EC aerosols using X-ray spectroscopy (XPS). We further assessed the effects of brands, power settings and nicotine concentration on the oxidation states of the detected metals.

2. Methods

We chose three popular EC brands available in the market as of 2021: JUUL (Juul pods, Juul Labs, USA), Vapor4Life (XL pen e-cig, AUTO VAPOR ZEUS KIT, Vapor4Life Inc., USA), and VOOPOO (Drag X, Shenzhen Woody Vapes Technology Co., China). These ECs were locally sourced for our research. JUUL and Vapor4Life brands employ pod-type (closed) systems, while the VOOPOO brand utilizes a mod-type system. The selection of EC brands was justified based on the design differences and device generations, with the VOOPOO representing the 3rd generation devices and the JUUL representing the 4th generation devices. We also assessed how power (5, 30, and 60W) and nicotine concentration (0 and 5 mg/ml) in the VOOPOO EC influenced the oxidation states of the emitted metals. The e-liquid used in this study contained 70% propylene glycol, 30% vegetable glycerin, and nicotine. Generally, nicotine salts are typically formed using weak acids, such as benzoic acid, lactic acid, or levulinic acid, even though the manufacturer did not disclose such information.[33] Control samples consisted of filters that were unexposed to EC aerosols. It is worth noting that, in light of considerable regulatory measures and rising public concern regarding ECs, the FDA imposed bans on Vapor4Life in 2021 and JUUL in 2022. Despite these bans, we included these brands in our

research for a comparative analysis, which could retrospectively examine the potential health impact associated with their usage and provide a general evaluation of pod-type systems.

Following our previously described protocol, we exposed EC aerosols to 37-mm-diameter Teflon filters (SKC Inc.).[11] Briefly, a computer-programmed flowmeter (Pneucleus Technologies LLC, Hollis, NH) was used to generate aerosols following the ISO 20768 standard puffing protocol: 55 mL puff volume, 3 s puff duration, and 30 s puff interval. The detailed description of the puff profile meeting ISO 20768 specifications has been included in the supplementary information. Thirty puffs of aerosol samples were collected from each EC configuration, and the filter was carefully removed, cut into 1 cm^2, and analyzed with the XPS. The XPS data were collected using a VG ESCALAB 220i-XL electron spectrometer (VG Scientific Ltd., UK). Monochromatic Al Kα X-rays (1486.7 eV) were employed. Typical operating conditions for the X-ray source were 400-μm nominal X-ray spot size (FWHM) operating at 15 kV, 8.9 mA, and 120 W for both survey and high-resolution spectra. A 2-micron-thick aluminum window was used to isolate the X-ray chamber from the sample analysis chamber to prevent high-energy electrons from impinging on the sample. Survey spectra, from 0 to 1200 eV binding energy, were collected at 100 eV pass energy with an energy resolution of ~1.0 eV, a dwell time of 100 ms, and two scans averaged. High-resolution spectra were collected at a pass energy of 20 eV, energy resolution of ~0.1 eV, dwell time of 100 ms, and 10 scans averaged in the respective binding energy range. Data acquisition and processing were performed using the Eclipse data system software. The operating pressure of the spectrometer was typically 10^{-9} mbar. An electron flood gun was used to compensate for the sample charging. The carbon 1S was first scanned to calibrate the instrument, and at least ten replicates were conducted for each sample.

3. Results and Discussion

3.1. Oxidation states of metals in EC aerosols and e-liquid

The XPS spectra of the elements detected on the filters exposed to EC aerosols from the VOOPOO brand (30W) and e-liquid are shown in **Fig. 1a**. Several non-metallic elements, mainly Teflon filter constituents and dense ambient elements (C, F, and O), can be observed on the filters exposed to both EC aerosols and the e-liquid. Metals were detected on filters exposed to EC aerosols, including Cr, Cu, Ni, Pb, and Zn, in all the tested brands. It is worth mentioning that metals with surface concentrations below 0.1%, such as Mn, are not included in the discussion. **Fig. 1b** shows the XPS survey spectra of the elements detected on the filters that collect aerosols generated by different brands of EC. Several trace metals were exclusive to specific brands, such as Sn for Vapor4Life, and Ni and Ba for JUUL.

Our previous study used inductively coupled plasma mass spectrometry (ICP-MS) to observe different quantities of metals emitted in EC aerosols.[11] Therefore, the current study provides additional details by confirming their electronic states via metals' core electron levels, notably Cu*2p*, Cr*2p*, Pb*4f*, Pb*5d* and Zn*2p*. Most detected metals are from EC components, hinting that these metals emanate from the heating coil or other metal components such as the mouthpiece and the wick.[6] All tested EC brands exhibited similar metal oxidation states.

Fig. 2 illustrates typical high-resolution spectra of the detected metals, which can be used to analyze the oxidation states of the five primary (abundant) metals emitted from EC aerosols of VOOPOO brand: Cr (**Fig. 2a**), Cu (**Fig. 2b**), Ni (**Fig. 2c**), Zn (**Fig. 2d**), and Pb (**Fig. 2e**). Particularly, the deconvoluted Cr$2p_{3/2}$ peak exhibited a signal at 577 eV, indicating the presence of Cr (III) (**Fig. 2a**). Another peak was observed at 572.7 eV, this value is somewhat lower than what would typically be expected for either Cr (III) or Cr (VI). This could be due to factors such

as the presence of Cr-ligands bonds.[34] Evidence is mounting that Cr (III) is genotoxic,[35] thus highlighting the need to monitor total Cr levels, as reported in previous studies, including the low Occupational Safety and Health Administration permissible exposure limit of 0.5 mg/m³ for 8-hour time-weighted average.[5,6,9,11]

In **Fig. 2b**, a distinct Cu species signal was detected at 932.9 eV, which likely corresponds to Cu (II) given a weak satellite peak around 943 eV. Cu (II) species have been shown to exhibit greater DNA-binding affinity than other divalent cations, thereby promoting DNA oxidation even at lower concentrations.[36] Elevated Cu concentrations may promote cancer development by damaging DNA with free hydroxyl radicals. In **Fig. 2c**, a satellite peak of the deconvoluted Ni$2p_{3/2}$ was observed at 861.9 eV, indicating a complex formed by the interaction between e-liquid's derived ligands, likely organic molecules derived from nitrogen-containing compounds or more importantly as recently reported, from certain chelating acids such as lactic acid from the nicotine salts,[33] and nickel. Another peak was observed at 854.4 eV, suggesting Ni (II) oxide species. Ni (II) species can produce superoxide anions from diatomic molecules and free radicals. Superoxide anions combine with protons to dismutate hydrogen peroxide, causing Ni-induced pathophysiological alterations in biological systems.[37,38] Nichrome or stainless steel, commonly used as EC heating coils, has been proposed as a potential source of these metallic species, with evidence supporting stainless steel while nichrome supposition is still under investigation. The main Zn$2p_{3/2}$ was observed at 1022.3 eV (**Fig 2d),** corresponding to Zn (II). Exposure to Zn oxides, with primary Zn (II) species, has been proven to induce acute inhalation toxicity in mice and may have detrimental implications in humans.[39,40] Pb species were detected at three binding energies. **Fig. 2e** displays the Pb$4f_{7/2}$ peak deconvoluted at 138.6 eV and 139.8 eV, corresponding to Pb (II) and Pb (IV), respectively. The Pb$4f_{5/2}$ component is also observed at

approximately 143.6 eV, suggesting Pb (II) species. Pb species are highly toxic when inhaled and can cause harm to several body systems, such as cognitive impairment, kidney damage, and nausea, even at low concentrations, as the metal is more readily absorbed through the lungs and into the bloodstream.[41]

Collectively, the XPS analyses of the filters exposed to EC aerosols reveal the oxidation states of the metals emitted by EC aerosols. Importantly, the results showed that the metal species were generally in the less toxic oxidation states (**Table 1**), and none were pure metals. This information is essential as it informs the existence of metal species of differential toxicity and thus considers the metal species-specific contribution to vaping use-associated lung injury.[42–44]

3.2.Effect of power settings and nicotine concentration on oxidation states

We analyzed the XPS survey spectrum from the filters exposed to VOOPOO EC aerosols under the following conditions: power settings at 5, 30, and 60 W; nicotine concentrations in the e-liquid of 0 mg/ml and 5 mg/ml (nicotine strengths used as specified by the e-liquid manufacturer). **Fig. 3** shows distinct peaks corresponding to various elements (Cu, Cr, Zn, and O). The Cu*2p* peak appears at approximately 932 eV, indicating the presence of Cu. Similarly, the Zn*2p* peak is located around 1021 eV. The Cr*2p* peak is located at approximately 574 eV while the Pb$4f_{7/2}$ is around 138 eV. Comparative analysis of the spectra from the samples exposed to different conditions reveals negligible trends (peak intensities were statistically analyzed and found not to vary significantly across different testing conditions). The intensities of the Cu$2p_{3/2}$ and Zn*2p* peaks are observed to be similar in the spectra of samples treated with 5 or 60W (**Fig. 3a**) and in those exposed to 0 mg/mL or 5 mg/mL nicotine e-liquid (**Fig. 3b**). In addition to the metal peaks, the spectra also exhibit several peaks corresponding to the elemental

composition of nicotine and the polytetrafluoroethylene filter. These include peaks for carbon (C), nitrogen (N), oxygen (O), and fluorine (F), reflecting the complex chemical composition of the analyzed samples. The presence of nicotine could alter the thermal degradation pathway of the e-liquid, leading to changes in the metal emission profile.[11] However, our results suggest no alteration of oxidation states.

Fig. 4 shows the influence of different EC power settings on the high-resolution spectra of the metals detected on exposed filters. A noticeable change was observed for Cr deconvolution of the Cr peak, indicating a change in the Cr (III) oxidation states (Fig. 4a) between 5 and 30W EC power settings, likely due to ligands.[33] However, under 60W, the Cr$2p_{3/2}$ core level could be deconvoluted into three peaks at 579.4 eV, 576.9 eV and 572.6 eV. The latter peak can be attributed to the presence of different oxidation states associated with chromium compounds or ligands, or it can be attributed to noise caused by Zn, whereas the former peak indicates the presence of about 15% of Cr (VI) species.[34,45]The power setting of the device directly influences the temperature reached by the heating coil.[46,47] At higher power settings (60 W), the presence of 15% Cr (VI) suggests that the high coil temperature and potentially the contribution of other ions such as alkali, is sufficient to trigger Cr (VI) oxide formation.[48] This aligns with the temperature-dependent nature of chromate formation.

Cu and Zn oxidation states and species distributions show minimal difference at different power settings of the EC device (**Fig. 4b** and **Fig. 4c**, respectively). In **Fig. 4d**, the high-resolution spectra of Ni$2p_{3/2}$ reveal distinct features at different power settings. At 5W, a peak at 861.5 eV is prominent, indicating the satellite of Ni$2p_{1/2}$ orbital at a higher binding energy. The presence of this species indicates that Ni (II) is in a complex ligand environment made of e-liquid constituents (e.g., organic molecules derived from nitrogen-containing compounds).[49–51]

This complex is likely formed due to the interaction of Ni (II) species with the various constituents in the e-liquid, such as PG, VG, nicotine, and flavorings. The complexation of Ni (II) with these ligands can alter its electronic structure, leading to a shift in the binding energy of the Ni peak from its expected value for Ni (II) in the free state. When the EC was operated at 30W and 60W, the peaks at 854.4 and 853.6 eV became evident, suggesting the impact of the resulting higher temperatures on Ni-ligands interactions. At higher power settings, ECs operate at increased temperatures, leading to vaporization and potentially causing chemical transformations of the e-liquid constituents.[52,53] The peak's presence at both 30W and 60W but not at lower wattages suggests a particular range of energy input conducive to this specific Ni-ligand interaction. Further analysis of the e-liquid composition and its interaction with Ni (II) under thermal conditions can provide more insights into the nature of this complex ligand environment.

Overall, we hereby report a second oxidation state for chromium (Cr (VI)) at higher power in addition to Cr (III) observed in all other conditions. The temperature of the heating coil is affected by the EC's power settings and has been proven to affect metal emissions.[11,54] For instance, when the EC voltage was raised from 2.2 to 5.7 V, the coil temperature rose from 106.8 to 265.8 °C.[55] Thus, increasing device power may accelerate coil breakdown and related metal emissions. Our results also show that the oxidation states of Cu, Ni, and Zn were not significantly affected by the nicotine concentration and device brand. It is generally understood that the oxidation states of metals can undergo alterations at temperatures between 350 and 800 °C, depending on the metal.[56,57] Given this property, it is plausible that the temperatures achieved at the devices' heating coils at the 60W setting might have fallen within this critical temperature range, influencing the observed variety in the oxidation states of Cr.

While this study analyzed a few popular EC brands to determine the oxidation states of metals in their emitted aerosols, it is crucial to note that these brands cannot represent the entire EC market's fast-evolving landscape. Different EC brands may utilize varying materials or employ distinct heating mechanisms, potentially leading to diverse metal emission profiles. Therefore, our findings should be interpreted cautiously as they represent the analyzed brands and may not universally apply to all ECs. In addition, the aerosol collection methodology employed in this study involved specific conditions and settings that may not fully replicate real-world EC usage or smoking behaviors. Factors such as puff duration, volume, and frequency, which can vary significantly among users, were standardized in our experimental setup. Future studies could aim to replicate a more diverse array of usage patterns to capture a broader range of emission profiles or involve human subjects to quantify the emission and impact of these metals from ECs. Finally, we focused on analyzing specific metals known to be present in EC aerosols, such as Ni, Cr, and Cu, and the selection of these metals was based on their known health implications and their prevalence in EC aerosols, as reported by previous studies.[4,5,15,22] It is important to know that ECs can emit a wider range of metal species, including those not analyzed in this study. Further research could broaden the scope of metal analysis to include additional elements, providing a more holistic understanding of the potential health risks associated with EC aerosol exposure.

4. Conclusion

This study investigated the oxidation states of metals released from ECs using the X-ray photoelectron spectroscopy (XPS) analysis. Five metals (Cr, Cu, Ni, Pb, and Zn) were detected on the filters exposed to EC aerosols, and high-resolution spectra revealed their specific

oxidation states. We report that device brand and nicotine concentration did not influence metals' oxidation states. The results also indicated that changes in power settings affected the oxidation states of Cr in the EC aerosols. This observation suggests that the temperatures increase due to high power settings in the heating coil of the EC devices favors emission of varying metal oxidation states. Results further revealed that Cr exists predominantly in the Cr (III) state (nearly 100%) at low power settings (5W), while a notable amount (15%) of Cr (VI) is observed at higher power settings (60W). Cu, Zn, and Ni were exclusively present in the +2-oxidation state (Cu (II), Zn (II), and Ni (II), respectively). Although these metals are mostly in their less toxic oxidation states, it is essential to note that they may still pose potential risks to human health upon inhalation in large doses, depending on the frequency of usage for these devices. Further research is necessary to determine the toxicity and long-term health effects of metal inhalation from ECs.

Supporting Information. Detailed experimental setup, calibration data, flow rate and pressure measurements, and Figure S1 illustrating flow rate and pressure drop across the sampling filter.

Funding: This study is supported by the U.S. National Science Foundation (NSF) through Award 2204659. Y.W. is also partially supported by the NSF Award 2324142.

Competing interests: The authors have declared that no competing interests exist.

5. References

(1) Willershausen, I.; Wolf, T.; Weyer, V.; Sader, R.; Ghanaati, S.; Willershausen, B. Influence of E-Smoking Liquids on Human Periodontal Ligament Fibroblasts. *Head Face Med.* **2014**, *10* (1), 1–7. https://doi.org/10.1186/1746-160X-10-39.

(2) Gaur, S.; Agnihotri, R. Health Effects of Trace Metals in Electronic Cigarette Aerosols—a Systematic Review. *Biol. Trace Elem. Res.* **2019**, *188* (2), 295–315. https://doi.org/10.1007/s12011-018-1423-x.

(3) Samburova, V.; Bhattarai, C.; Strickland, M.; Darrow, L.; Angermann, J.; Son, Y.; Khlystov, A. Aldehydes in Exhaled Breath during E-Cigarette Vaping: Pilot Study Results. *Toxics* **2018**, *6* (3). https://doi.org/10.3390/toxics6030046.

(4) Pappas, R. S.; Gray, N.; Halstead, M.; Valentin-Blasini, L.; Watson, C. Toxic Metal-Containing Particles in Aerosols from Pod-Type Electronic Cigarettes. *J. Anal. Toxicol.* **2021**, *45* (4), 337–347. https://doi.org/10.1093/jat/bkaa088.

(5) Gray, N.; Halstead, M.; Gonzalez-Jimenez, N.; Valentin-Blasini, L.; Watson, C.; Pappas, R. S. Analysis of Toxic Metals in Liquid from Electronic Cigarettes. *Int. J. Environ. Res. Public Health* **2019**, *16* (22). https://doi.org/10.3390/ijerph16224450.

(6) Gray, N.; Halstead, M.; Valentin-Blasini, L.; Watson, C.; Pappas, R. S. Toxic Metals in Liquid and Aerosol from Pod-Type Electronic Cigarettes. *J. Anal. Toxicol.* **2022**, *46* (1), 69–75. https://doi.org/10.1093/jat/bkaa185.

(7) Khlystov, A.; Samburova, V. Flavoring Compounds Dominate Toxic Aldehyde Production during E-cigarette Vaping. *Environ. Sci. Technol.* **2016**, *50* (23), 13080–13085. https://doi.org/10.1021/acs.est.6b05145.

(8) Klager, S.; Vallarino, J.; MacNaughton, P.; Christiani, D. C.; Lu, Q.; Allen, J. G. Flavoring Chemicals and Aldehydes in E-Cigarette Emissions. *Environ. Sci. Technol.* **2017**, *51* (18), 10806–10813. https://doi.org/10.1021/acs.est.7b02205.

(9) Zhao, D.; Aravindakshan, A.; Hilpert, M.; Olmedo, P.; Rule, A. M.; Navas-Acien, A.; Aherrera, A. Metal/Metalloid Levels in Electronic Cigarette Liquids, Aerosols, and Human Biosamples: A Systematic Review. *Environ. Health Perspect.* **2020**, *128* (3). https://doi.org/10.1289/EHP5686.

(10) Pearce, K.; Gray, N.; Gaur, P.; Jeon, J.; Suarez, A.; Shannahan, J.; Pappas, R. S.; Watson-Wright, C. Toxicological Analysis of Aerosols Derived from Three Electronic Nicotine Delivery Systems Using Normal Human Bronchial Epithelial Cells. *Toxicol. Vitr.* **2020**, *69* (July), 104997. https://doi.org/10.1016/j.tiv.2020.104997.

(11) Fabrice Kapiamba, K.; Hao, W.; Adom, S.; Liu, W.; Huang, Y.-W.; Wang, Y. Examining Metal Contents in Primary and Secondhand Aerosols Released by Electronic Cigarettes. *Chem. Res. Toxicol.* **2022**, *35* (6), 954–962. https://doi.org/10.1021/acs.chemrestox.1c00411.

(12) Balali-Mood, M.; Naseri, K.; Tahergorabi, Z.; Khazdair, M. R.; Sadeghi, M. Toxic Mechanisms of Five Heavy Metals: Mercury, Lead, Chromium, Cadmium, and Arsenic.

Front. Pharmacol. **2021**, *12* (April), 1–19. https://doi.org/10.3389/fphar.2021.643972.

(13) Sinicropi, M. S.; Amantea, D.; Caruso, A.; Saturnino, C. Chemical and Biological Properties of Toxic Metals and Use of Chelating Agents for the Pharmacological Treatment of Metal Poisoning. *Arch. Toxicol.* **2010**, *84* (7), 501–520. https://doi.org/10.1007/s00204-010-0544-6.

(14) Monsé, C.; Raulf, M.; Hagemeyer, O.; Van Kampen, V.; Kendzia, B.; Gering, V.; Marek, E. M.; Jettkant, B.; Bünger, J.; Merget, R.; Brüning, T. Airway Inflammation after Inhalation of Nano-Sized Zinc Oxide Particles in Human Volunteers. *BMC Pulm. Med.* **2019**, *19* (1), 1–11. https://doi.org/10.1186/s12890-019-1026-0.

(15) Xing, W.; Zhao, Q.; Scheckel, K. G.; Zheng, L.; Li, L. Inhalation Bioaccessibility of Cd, Cu, Pb and Zn and Speciation of Pb in Particulate Matter Fractions from Areas with Different Pollution Characteristics in Henan Province, China. *Ecotoxicol. Environ. Saf.* **2019**, *175* (February), 192–200. https://doi.org/10.1016/j.ecoenv.2019.03.062.

(16) Rossner, P.; Vrbova, K.; Rossnerova, A.; Zavodna, T.; Milcova, A.; Klema, J.; Vecera, Z.; Mikuska, P.; Coufalik, P.; Capka, L.; Krumal, K.; Docekal, B.; Holan, V.; Machala, M.; Topinka, J. Gene Expression and Epigenetic Changes in Mice Following Inhalation of Copper(II) Oxide Nanoparticles. *Nanomaterials* **2020**, *10* (3). https://doi.org/10.3390/nano10030550.

(17) Hejazy, M.; Koohi, M. K.; Pour, A. B. M.; Najafi, D. Toxicity of Manufactured Copper Nanoparticles - A Review. *Nanomedicine Res. J.* **2018**, *3* (1), 1–9. https://doi.org/10.22034/NMRJ.2018.01.001.

(18) Tulinska, J.; Mikusova, M. L.; Liskova, A.; Busova, M.; Masanova, V.; Uhnakova, I.; Rollerova, E.; Alacova, R.; Krivosikova, Z.; Wsolova, L.; Dusinska, M.; Horvathova, M.; Szabova, M.; Lukan, N.; Stuchlikova, M.; Kuba, D.; Vecera, Z.; Coufalik, P.; Krumal, K.; Alexa, L.; Vrlikova, L.; Buchtova, M.; Dumkova, J.; Piler, P.; Thon, V.; Mikuska, P. Copper Oxide Nanoparticles Stimulate the Immune Response and Decrease Antioxidant Defense in Mice After Six-Week Inhalation. *Front. Immunol.* **2022**, *13* (April), 1–12. https://doi.org/10.3389/fimmu.2022.874253.

(19) Zhong, L.; Liu, X.; Hu, X.; Chen, Y.; Wang, H.; Lian, H. zhen. In Vitro Inhalation Bioaccessibility Procedures for Lead in PM2.5 Size Fraction of Soil Assessed and Optimized by in Vivo-in Vitro Correlation. *J. Hazard. Mater.* **2020**, *381* (August 2019), 121202. https://doi.org/10.1016/j.jhazmat.2019.121202.

(20) Vysloužil, J.; Kulich, P.; Zeman, T.; Vaculovič, T.; Tvrdoňová, M.; Mikuška, P.; Večeřa, Z.; Stráská, J.; Moravec, P.; Balcar, V. J.; Šerý, O. Subchronic Continuous Inhalation Exposure to Zinc Oxide Nanoparticles Induces Pulmonary Cell Response in Mice. *J. Trace Elem. Med. Biol.* **2020**, *61* (February), 0–9. https://doi.org/10.1016/j.jtemb.2020.126511.

(21) Monsé, C.; Hagemeyer, O.; van Kampen, V.; Raulf, M.; Weiss, T.; Menne, E.; Jettkant, B.; Kendzia, B.; Merget, R.; Brüning, T.; Bünger, J. Human Inhalation Study with Zinc Oxide: Analysis of Zinc Levels and Biomarkers in Exhaled Breath Condensate. *Adv. Exp. Med. Biol.* **2021**, *1324* (August), 83–90. https://doi.org/10.1007/5584_2020_572.

(22) Alriksson, S.; Voxberg, E.; Karlsson, H.; Ljunggren, S.; Augustsson, A. Temporal Risk Assessment – 20th Century Pb Emissions to Air and Exposure via Inhalation in the Swedish Glass District. *Sci. Total Environ.* **2023**, *858* (October 2022), 159843. https://doi.org/10.1016/j.scitotenv.2022.159843.

(23) Sengul, A. B.; Asmatulu, E. Toxicity of Metal and Metal Oxide Nanoparticles: A Review. *Environ. Chem. Lett.* **2020**, *18* (5), 1659–1683. https://doi.org/10.1007/s10311-020-01033-6.

(24) Jaishankar, M.; Tseten, T.; Anbalagan, N.; Mathew, B. B.; Beeregowda, K. N. Toxicity, Mechanism and Health Effects of Some Heavy Metals. *Interdiscip. Toxicol.* **2014**, *7* (2), 60–72. https://doi.org/10.2478/intox-2014-0009.

(25) Sjekhawat, K. C. S. J. B. Chromium Toxicity and Its Health Hazards. *Int. J. Adv. Res.* **2015**, *3* (7), 167–172.

(26) Liang, J.; Huang, X.; Yan, J.; Li, Y.; Zhao, Z.; Liu, Y.; Ye, J.; Wei, Y. A Review of the Formation of Cr(VI) via Cr(III) Oxidation in Soils and Groundwater. *Sci. Total Environ.* **2021**, *774*, 145762. https://doi.org/10.1016/j.scitotenv.2021.145762.

(27) Tsuchiyama, F.; Hisanaga, N.; Shibata, E.; Aoki, T.; Takagi, H.; Ando, T.; Takeuchi, Y. Pulmonary Metal Distribution in Urban Dwellers. *Int. Arch. Occup. Environ. Health* **1997**, *70* (2), 77–84. https://doi.org/10.1007/s004200050190.

(28) Sun, H.; Brocato, J.; Costa, M. Oral Chromium Exposure and Toxicity. *Curr. Environ. Heal. reports* **2015**, *2* (3), 295–303. https://doi.org/10.1007/s40572-015-0054-z.

(29) Reaney, S. H.; Kwik-uribe, C. L.; Smith, D. R. Manganese Oxidation State and Its Implications for Toxicity. *Chem. Res. Toxicol.* **2002**, *15* (Iii), 1119–1126.

(30) Gunter, T. E.; Miller, L. M.; Gavin, C. E.; Eliseev, R.; Salter, J.; Buntinas, L.; Alexandrov, A.; Hammond, S.; Gunter, K. K. Determination of the Oxidation States of Manganese in Brain, Liver, and Heart Mitochondria. *J. Neurochem.* **2004**, *88* (2), 266–280. https://doi.org/10.1046/j.1471-4159.2003.02122.x.

(31) Ashish, B.; Neeti, K.; Himanshu, K. Copper Toxicity: A Comprehensive Study. *Res. J. Recent Sci.* **2013**, *2* (ISC-2012), 58–67.

(32) Beswick, P. H.; Hall, G. H.; Hook, A. J.; Little, K.; McBrien, D. C. H.; Lott, K. A. K. Copper Toxicity: Evidence for the Conversion of Cupric to Cuprous Copper in Vivo under Anaerobic Conditions. *Chem. Biol. Interact.* **1976**, *14* (3–4), 347–356. https://doi.org/10.1016/0009-2797(76)90113-7.

(33) Pappas, R. S.; Gray, N.; Halstead, M.; Watson, C. H. Lactic Acid Salts of Nicotine Potentiate the Transfer of Toxic Metals into Electronic Cigarette Aerosols. *Toxics* **2024**, *12* (1). https://doi.org/10.3390/toxics12010065.

(34) Briggs, D. X-Ray Photoelectron Spectroscopy (XPS). *Handb. Adhes. Second Ed.* **2005**, 621–622. https://doi.org/10.1002/0470014229.ch22.

(35) Fang, Z.; Zhao, M.; Zhen, H.; Chen, L.; Shi, P.; Huang, Z. Genotoxicity of Tri- and Hexavalent Chromium Compounds in Vivo and Their Modes of Action on DNA Damage

in Vitro. *PLoS One* **2014**, *9* (8). https://doi.org/10.1371/journal.pone.0103194.

(36) Theophanides, T.; Anastassopoulou, J. Copper and Carcinogenesis. *Crit. Rev. Oncol. Hematol.* **2002**, *42* (1), 57–64. https://doi.org/10.1016/S1040-8428(02)00007-0.

(37) Das, K. K.; Reddy, R. C.; Bagoji, I. B.; Das, S.; Bagali, S.; Mullur, L.; Khodnapur, J. P.; Biradar, M. S. Primary Concept of Nickel Toxicity - An Overview. *J. Basic Clin. Physiol. Pharmacol.* **2019**, *30* (2), 141–152. https://doi.org/10.1515/jbcpp-2017-0171.

(38) Begum, W.; Rai, S.; Banerjee, S.; Bhattacharjee, S.; Mondal, M. H.; Bhattarai, A.; Saha, B. A Comprehensive Review on the Sources, Essentiality and Toxicological Profile of Nickel. *RSC Adv.* **2022**, *12* (15), 9139–9153. https://doi.org/10.1039/d2ra00378c.

(39) Larsen, S. T.; Da Silva, E.; Hansen, J. S.; Jensen, A. C. Ø.; Koponen, I. K.; Sørli, J. B. Acute Inhalation Toxicity After Inhalation of ZnO Nanoparticles: Lung Surfactant Function Inhibition In Vitro Correlates With Reduced Tidal Volume in Mice. *Int. J. Toxicol.* **2020**, *39* (4), 321–327. https://doi.org/10.1177/1091581820933146.

(40) Vimercati, L.; Cavone, D.; Caputi, A.; De Maria, L.; Tria, M.; Prato, E.; Ferri, G. M. Nanoparticles: An Experimental Study of Zinc Nanoparticles Toxicity on Marine Crustaceans. General Overview on the Health Implications in Humans. *Front. Public Heal.* **2020**, *8* (May), 1–19. https://doi.org/10.3389/fpubh.2020.00192.

(41) Arsenic, Metals, Fibres and Dusts. *IARC Monographs on the Evaluation of Carcinogenic Risks to Humans*. IARC Press, International Agency for Research on Cancer : Lyon 2012, p xi + 501 pp.

(42) Donaldson, K.; Stone, V.; Gilmour, P. S.; Brown, D. M.; Macnee, W. Ultrafine Particles: Mechanisms of Lung Injury. *Philos. Trans. R. Soc. A Math. Phys. Eng. Sci.* **2000**, *358* (1775), 2741–2749. https://doi.org/10.1098/rsta.2000.0681.

(43) Gonzalez-Jimenez, N.; Gray, N.; Pappas, R. S.; Halstead, M.; Lewis, E.; Valentin-Blasini, L.; Watson, C.; Blount, B. Analysis of Toxic Metals in Aerosols from Devices Associated with Electronic Cigarette, or Vaping, Product Use Associated Lung Injury. *Toxics* **2021**, *9* (10). https://doi.org/10.3390/toxics9100240.

(44) Kunimasa, K.; Arita, M.; Tachibana, H.; Tsubouchi, K.; Konishi, S.; Korogi, Y.; Nishiyama, A.; Ishida, T. Chemical Pneumonitis and Acute Lung Injury Caused by Inhalation of Nickel Fumes. *Intern. Med.* **2011**, *50* (18), 2035–2038. https://doi.org/10.2169/internalmedicine.50.5557.

(45) Son, B. K.; Choi, J. W.; Jeon, S. B.; Son, I. Zn–Ni Alloy Plating with Trivalent Chromate: Effects of NaF Additive Concentration and Treatment Time on Film Color, Thickness, and Electrochemical Properties. *Coatings* **2022**, *12* (8). https://doi.org/10.3390/coatings12081160.

(46) Chen, W.; Wang, P.; Ito, K.; Fowles, J.; Shusterman, D.; Jaques, P. A.; Kumagai, K. Measurement of Heating Coil Temperature for E-Cigarettes with a "Top-Coil" Clearomizer. *PLoS One* **2018**, *13* (4), 1–16. https://doi.org/10.1371/journal.pone.0195925.

(47) Mulder, H. A.; Stewart, J. B.; Blue, I. P.; Krakowiak, R. I.; Patterson, J. L.; Karin, K. N.; Royals, J. M.; DuPont, A. C.; Forsythe, K. E.; Poklis, J. L.; Poklis, A.; Butler, S. N.;

Turner, J. B. M. G.; Peace, M. R. Characterization of E-Cigarette Coil Temperature and Toxic Metal Analysis by Infrared Temperature Sensing and Scanning Electron Microscopy–Energy-Dispersive X-Ray. *Inhal. Toxicol.* **2020**, *32* (13–14), 447–455. https://doi.org/10.1080/08958378.2020.1840678.

(48) Verbinnen, B.; Billen, P.; Van Coninckxloo, M.; Vandecasteele, C. Heating Temperature Dependence of Cr(III) Oxidation in the Presence of Alkali and Alkaline Earth Salts and Subsequent Cr(VI) Leaching Behavior. *Environ. Sci. Technol.* **2013**, *47* (11), 5858–5863. https://doi.org/10.1021/es4001455.

(49) Pandey, D. K.; Ankade, S. B.; Ali, A.; Vinod, C. P.; Punji, B. Nickel-Catalyzed C-H Alkylation of Indoles with Unactivated Alkyl Chlorides: Evidence of a Ni(i)/Ni(Iii) Pathway. *Chem. Sci.* **2019**, *10* (41), 9493–9500. https://doi.org/10.1039/c9sc01446b.

(50) Grosvenor, A. P.; Biesinger, M. C.; Smart, R. S. C.; McIntyre, N. S. New Interpretations of XPS Spectra of Nickel Metal and Oxides. *Surf. Sci.* **2006**, *600* (9), 1771–1779. https://doi.org/10.1016/j.susc.2006.01.041.

(51) Mehmood, S.; Zhao, X.; Fahad Bhopal, M.; Ullah Khan, F.; Yang, Y.; Wang, G.; Pan, X. MoO2-Ni-Graphene Ternary Nanocomposite for a High- Performance Room-Temperature Ethanol Gas Sensor. *Appl. Surf. Sci.* **2021**, *554* (February), 149595. https://doi.org/10.1016/j.apsusc.2021.149595.

(52) Jaegers, N. R.; Hu, W.; Weber, T. J.; Hu, J. Z. Low-Temperature (< 200 °C) Degradation of Electronic Nicotine Delivery System Liquids Generates Toxic Aldehydes. *Sci. Rep.* **2021**, *11* (1), 1–12. https://doi.org/10.1038/s41598-021-87044-x.

(53) Li, Y.; Burns, A. E.; Tran, L. N.; Abellar, K. A.; Poindexter, M.; Li, X.; Madl, A. K.; Pinkerton, K. E.; Nguyen, T. B. Impact of E-Liquid Composition, Coil Temperature, and Puff Topography on the Aerosol Chemistry of Electronic Cigarettes. *Chem. Res. Toxicol.* **2021**, *34* (6), 1640–1654. https://doi.org/10.1021/acs.chemrestox.1c00070.

(54) Zhao, D.; Navas-Acien, A.; Ilievski, V.; Slavkovich, V.; Olmedo, P.; Adria-Mora, B.; Domingo-Relloso, A.; Aherrera, A.; Kleiman, N. J.; Rule, A. M.; Hilpert, M. Metal Concentrations in Electronic Cigarette Aerosol: Effect of Open-System and Closed-System Devices and Power Settings. *Environ. Res.* **2019**, *174* (March), 125–134. https://doi.org/10.1016/j.envres.2019.04.003.

(55) Zhao, J.; Nelson, J.; Dada, O.; Pyrgiotakis, G.; Kavouras, I. G.; Demokritou, P. Assessing Electronic Cigarette Emissions: Linking Physico-Chemical Properties to Product Brand, e-Liquid Flavoring Additives, Operational Voltage and User Puffing Patterns. *Inhal. Toxicol.* **2018**, *30* (2), 78–88. https://doi.org/10.1080/08958378.2018.1450462.

(56) Carley, A. F.; Jackson, S. D.; O'Shea, J. N.; Roberts, M. W. Oxidation States at Alkali-Metal-Doped Ni(110)-O Surfaces. *Phys. Chem. Chem. Phys.* **2001**, *3* (2), 274–281. https://doi.org/10.1039/b006718k.

(57) Chan, W. T. K.; Wong, W. T. A Brief Introduction to Transition Metals in Unusual Oxidation States. *Polyhedron* **2013**, *52*, 43–61. https://doi.org/10.1016/j.poly.2012.09.004.

Tables and Figures

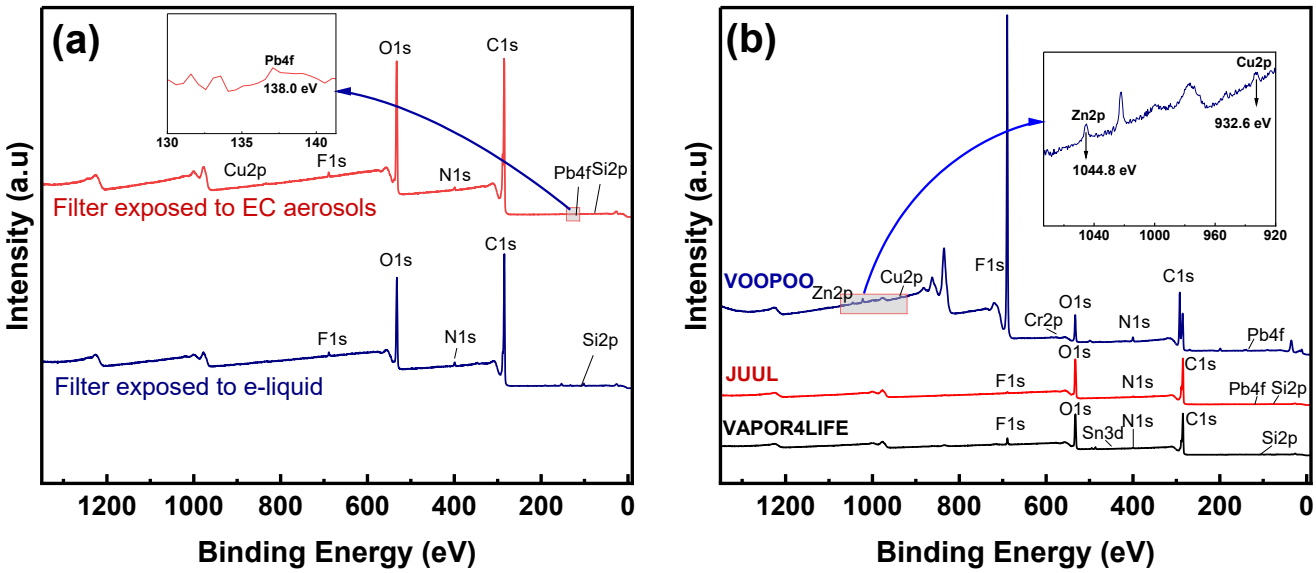

Fig. 1 XPS survey spectra showing chemical species observed on: (a) filters exposed to EC aerosol and e-liquid, (b) filters exposed to 30 puffs of aerosols from three different EC brands (VOOPOO operated at 30W, JUUL and VAPOR4LIFE used at default settings). We observed these metals from the ICP-MS analysis of the exposed filters that were reported in our previous study. [11]

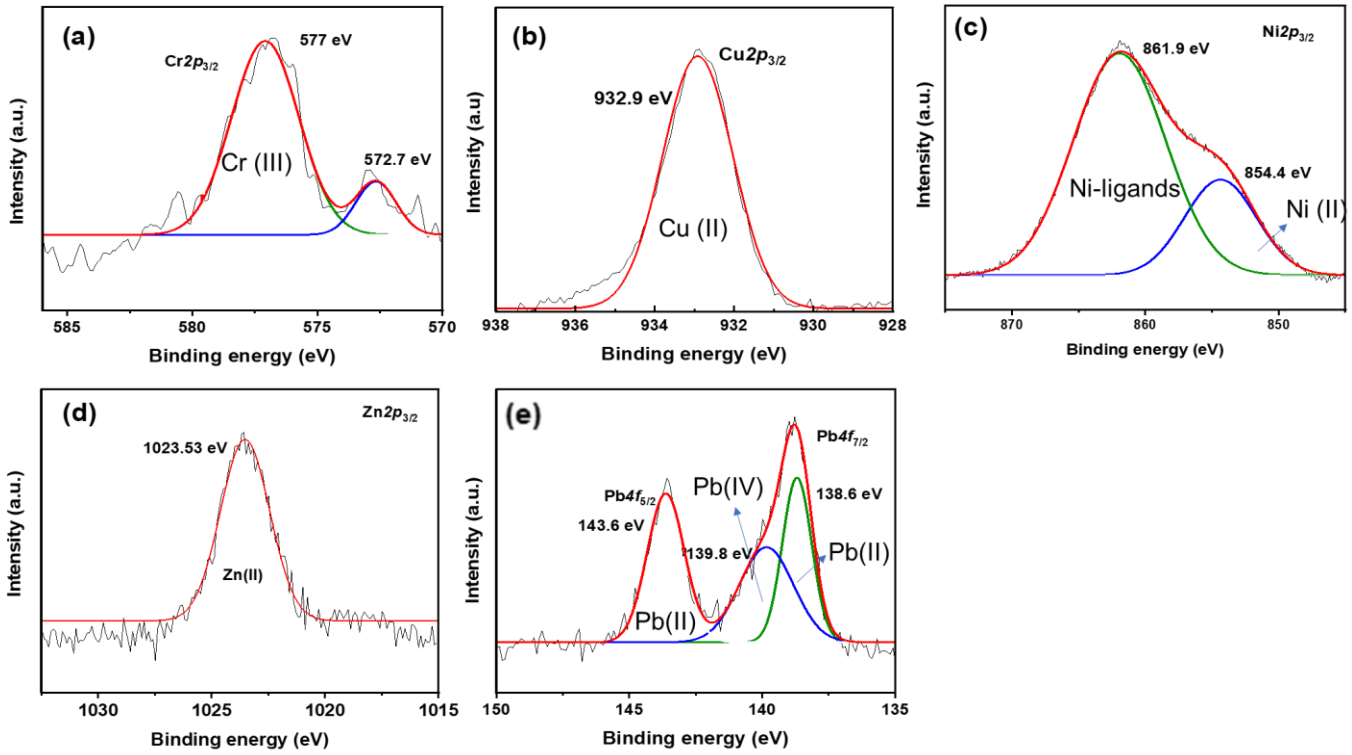

Fig. 2 High-resolution XPS spectra of selected metals with consistently higher concentrations on the surface of the filter exposed to EC aerosol's (VOOPOO, 60W): (a) Cr*2p*, (b) Cu*2p*, (c) Ni*2p*, (d) Zn*2p*, and (e) Pb*4f*

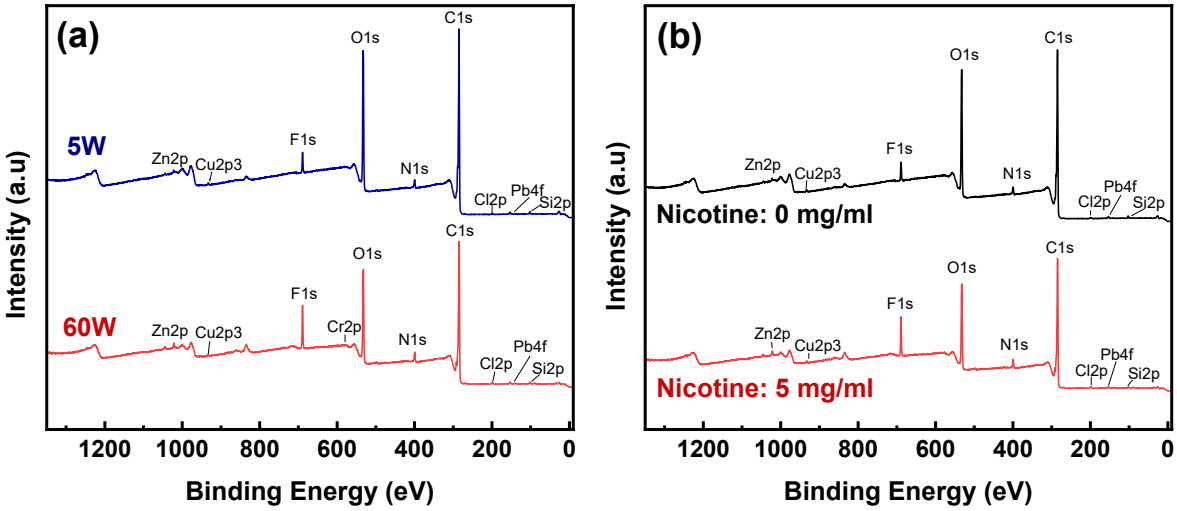

Fig. 3 XPS survey (Normalized intensity) of emitted metals from the VOOPOO device in response to (a) EC power settings and (b) nicotine concentration in the e-liquid

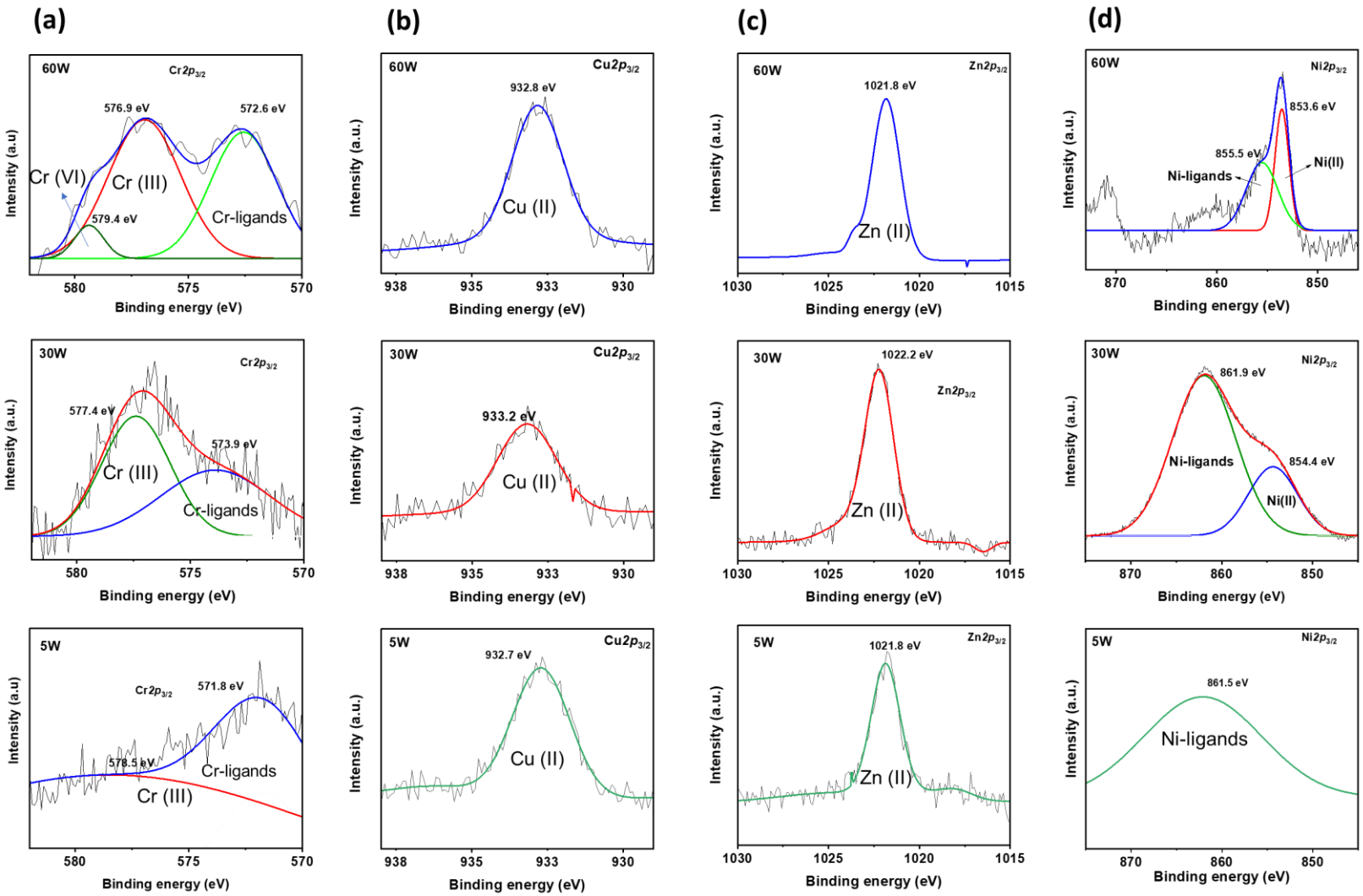

Fig. 4 High-resolution XPS spectra (with normalized intensity) of selected metals on filter surfaces exposed to aerosols: (a) Cr*2p*, (b) Cu*2p*, (c) Zn*2p*, and (d) Ni*2p*. Three power settings (60, 30, and 5W) on the VOOPOO EC brand were tested

Table 1. Summary of distribution of the oxidation states of metals detected in EC aerosols with the EC cigarette operated at 60W. *Cr (VI) was only observed at 60W

Metal species	%
Cr (III)	100
Cr (VI)*	15*
Cu (II)	100
Ni (II)	100
Pb (II)	65
Pb (IV)	35
Zn (II)	100